The global potential for increased storage of carbon on land

Wayne S. Walker[a,1], Seth R. Gorelik[a], Susan C. Cook-Patton[b], Alessandro Baccini[c], Mary K. Farina[a], Kylen K. Solvik[d], Peter W. Ellis[b], Jon Sanderman[a], Richard A. Houghton[a], Sara M. Leavitt[b], Christopher R. Schwalm[a], and Bronson W. Griscom[e]

Constraining the climate crisis requires urgent action to reduce anthropogenic emissions while simultaneously removing carbon dioxide from the atmosphere. Improved information about the maximum magnitude and spatial distribution of opportunities for additional land-based removals of CO_2 is needed to guide on-the-ground decision-making about where to implement climate change mitigation strategies. Here, we present a globally consistent spatial dataset (approximately 500-m resolution) of current, potential, and unrealized potential carbon storage in woody plant biomass and soil organic matter. We also provide a framework for prioritizing actions related to the restoration, management, and maintenance of woody carbon stocks and associated soils. By comparing current to potential carbon storage, while excluding areas critical to food production and human habitation, we find 287 petagrams (PgC) of unrealized potential storage opportunity, of which 78% (224 PgC) is in biomass and 22% (63 PgC) is in soil. Improved management of existing forests may offer nearly three-fourths (206 PgC) of the total unrealized potential, with the majority (71%) concentrated in tropical ecosystems. However, climate change is a source of considerable uncertainty. While additional research is needed to understand the impact of natural disturbances and biophysical feedbacks, we project that the potential for additional carbon storage in woody biomass will increase (+17%) by 2050 despite projected decreases (−12%) in the tropics. Our results establish an absolute reference point and conceptual framework for national and jurisdictional prioritization of locations and actions to increase land-based carbon storage.

natural climate solutions | negative emissions | forest maintenance | improved forest management | forest restoration

Emissions of carbon to the atmosphere must remain below ∼250 petagrams (PgC) (918 PgCO2) from 2021 onward to achieve the Paris Agreement's goal of limiting global temperature rise to well below 2 °C (1–3). At present rates, that amount of carbon will be emitted by 2045. It follows that even necessary and drastic cuts in emissions (i.e., a rapid transition from fossil fuels to renewable energy sources) must be accompanied by carbon dioxide removal (CDR) or negative emissions strategies (4). Promising options for large-scale CDR include improved land stewardship (5), commonly referred to as natural climate solutions (NCS) (6–8). In particular, increasing carbon storage in woody biomass (e.g., forest ecosystems) is widely recognized as having high climate mitigation potential while also affording an array of environmental and socio-economic cobenefits (6–9). While a growing body of research has estimated the near-term potential for land-based climate mitigation (6, 8, 10), these studies emphasize the climate benefit over short, 10- to 30-y planning horizons. They do not include estimates of the upper limit for additional land-based carbon storage or its spatial distribution. This information is essential for landscape-level planning and targeted implementation of NCS, given that the potential for additional carbon storage is necessarily defined by both the rate at which carbon can be sequestered and the magnitude of the available reservoir. Therefore, we provide 500-m-resolution global maps to quantify the maximum potential for additional carbon storage in ecosystems dominated by woody vegetation (i.e., trees and shrubs), under baseline (1960 to 1990) and future (representative concentration pathway scenario 8.5 [RCP8.5]) climate conditions. This information can be used to help direct NCS toward areas with the greatest maximum opportunity, inform when NCS will saturate, and identify the types of NCS actions that are best suited to a given location.

One approach to estimating maximum additional carbon storage—or the difference between current and potential carbon, which we term "unrealized potential" carbon—is a bookkeeping approach that tracks carbon fluxes through time. Under this approach, net land-based emissions since 1850 are estimated to have been 108 to 188 PgC, including both biomass (above and below ground) and soil organic matter (13–17). Estimates that account for preindustrial (i.e., pre-1850) land use are more

Significance

Despite increased interest in land-based carbon storage as a climate solution, there are physical limits on how much additional carbon can be incorporated into terrestrial ecosystems. To effectively determine where and how to act, jurisdictions need robust data illustrating the magnitude and distribution of opportunities to increase carbon storage, as well as information on the actions available to achieve that storage. Here, we provide globally consistent maps for directing additional carbon storage under current and future climate, as well as a framework for determining how that storage could be gained through restoration, improved management, or maintenance of woody biomass and soil organic matter. Our estimates provide an upper bound on how improved land stewardship can mitigate the climate crisis.

Author affiliations: [a]Woodwell Climate Research Center, Falmouth, MA 02540; [b]The Nature Conservancy, Arlington, VA 22203; [c]Department of Earth & Environment, Boston University, Boston, MA 02215; [d]Department of Geography, University of Colorado Boulder, Boulder, CO 80309; and [e]Conservation International, Arlington, VA 22202

[1]To whom correspondence may be addressed. Email: wwalker@woodwellclimate.org.

varied and increase post-1850 estimates by as much as 325 to 357 PgC (18) or as little as 48 to 153 PgC (11–13, 15). This high uncertainty limits the practical utility of this approach.

Other investigators have sought instead to quantify unrealized potential by comparing estimates of current and potential land carbon storage. Sanderman et al. (6), considering only soil organic carbon (SOC), estimated net losses in the upper 2 m of soil from agricultural land use to be 116 PgC since 10,000 BC. Erb et al. (19), focusing on changes in vegetation biomass, found losses in carbon due to human land use to be significantly larger (447 PgC) than the studies cited above that consider only the postindustrial period, but generally consistent with some of those that account for preindustrial human disturbance (18). Bastin et al. (20), in a study focused on the restoration of global tree cover, identified an additional reservoir of 206 PgC when considering all carbon pools (aboveground and belowground biomass, soil, litter, and dead wood) after excluding cropland and urban areas.

However, all of these global analyses fall short in delivering the robust spatially explicit information needed for targeted planning and implementation of landscape-level NCS. While the global dataset produced by Bastin et al. (20) has a reasonably high spatial resolution (30 arc seconds; approximately 900 m) and considers all land carbon pools, the product is limited to the storage potential afforded by the expansion of tree cover. Moreover, the result is subject to the uncertainty inherent in indirect estimates of carbon stock from area-based metrics of tree/forest cover (21). In comparison, the data product created by Erb et al. (19), which is based on several disparate yet direct estimates of terrestrial carbon storage, is limited by its treatment of only the biomass carbon pool and coarse spatial resolution (5 arc min; approximately 9.3 km). The authors themselves remark that "the uncertainty range could be narrowed if a single robust, validated method would be applied continuously in the stocktaking efforts" (19).

Here, we apply a consistent suite of methods to generate spatially explicit global estimates of current (ca. 2016) and climate-constrained potential land carbon storage in aboveground woody biomass (AGB), belowground woody biomass (BGB), and SOC pools at a spatial resolution of approximately 500 m. The difference between current and potential land carbon storage represents the unrealized potential for additional carbon accumulation in global woody biomass and soils. We then disaggregate this global estimate of unrealized potential carbon storage using a conceptual framework we term the NCS opportunity space: seven discrete, internally consistent, and spatially explicit categories of broad NCS action (Fig. 1). Categories are defined quantitatively in terms of woody carbon density, thereby avoiding the uncertainty associated with derivative approximations of potential carbon storage based on forest area or canopy cover. After applying safeguards to lands currently utilized for food production, human habitation (e.g., urban areas), and sensitive biodiversity (nonwoody grasslands), we demonstrate the utility of the opportunity space framework for landscape-level NCS planning by analyzing the global, regional, and national potential for additional land carbon storage attributable to restoration (e.g., reforestation), management (e.g., improved natural forest stewardship), and maintenance (i.e., the sequestration benefit accrued through avoided forest conversion) of woody carbon stocks and associated soils. Finally, we evaluate the uncertainty that climate change poses to the magnitude and spatial distribution of the unrealized potential for additional carbon storage through 2050.
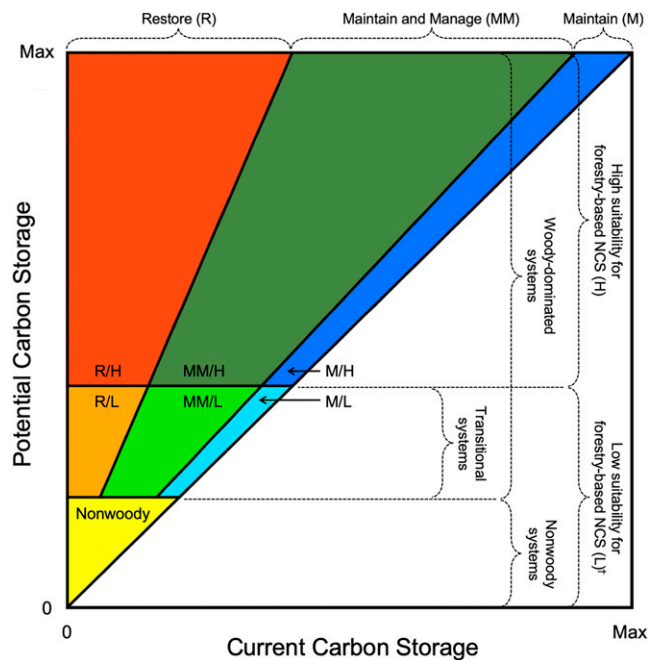

Fig. 1. The NCS opportunity space, consisting of seven categories defined by the ratio of current (x axis) to potential (y axis) carbon storage as well as carbon-based thresholds delineating NCS-relevant systems. Categories include: Restore/High suitability for forestry-based NCS (R/H; red), Maintain and manage/High suitability for forestry-based NCS (MM/H; dark green), Maintain/High suitability for forestry-based NCS (M/H; dark blue), Restore/Low suitability for forestry-based NCS (R/L; orange), Maintain and manage/Low suitability for forestry-based NCS (MM/L; light green), Maintain/Low suitability for forestry-based NCS (M/L; light blue), and Nonwoody (yellow). † denotes associated grassland/savanna biodiversity considerations.

Results

Unrealized Potential Carbon Storage: Unconstrained. Our map-based estimates of current (ca. 2016), potential, and unrealized potential carbon storage (SI Appendix, Fig. S1) indicate that current carbon storage in global woody biomass and soil (3,477.8 PgC) is at approximately 88% of its potential (3,971.9 PgC), revealing a 12% deficit or a total unrealized potential for additional land carbon storage of 494.2 PgC (Table 1). When considering biomass carbon alone (i.e., AGB + BGB), current storage (441.2 PgC; 321 to 659 PgC) represents just over half (55%) of the potential (795.5 PgC; 567 to 1,126 PgC) (Table 1). AGB alone represents more than half (56%, 274.4 PgC; 66 to 692 PgC) of the total unrealized potential, whereas BGB represents 16% (Table 1). In comparison, current storage in SOC (3,036.5 PgC) represents ~96% of the potential (3,176.4 PgC), reflecting the greater negative impact of historical land use on carbon storage in woody vegetation relative to soil (Table 1). Nevertheless, more than one-third (39%, 139.8 PgC) of unrealized potential carbon is in SOC (Table 1), underscoring 1) the substantial amount of carbon (3,036.5 PgC) currently stored in global soils, a value nearly 9 times that present above ground (349.1 PgC; 256 to 515 PgC), and 2) the amount of SOC that has been lost.

Unrealized Potential Carbon Storage: Constrained. We imposed spatial constraints on our map-based estimate of unrealized potential carbon storage (*SI Appendix*, Fig. S1) in recognition of the need to safeguard lands currently utilized for food production,

Table 1. Global current, potential, and unrealized potential carbon storage under baseline (1960 to 1990) and future (RCP8.5; mean and range of 11 Earth system models) climate scenarios.

	Biomass (PgC)			Soil (PgC)	Total (PgC)	
	AGB	BGB	AGB + BGB	SOC	AGB+BGB+ SOC$_b$	AGB+BGB+ SOC
Walker et al. (this study)						
Baseline climate (1960–1990)						
Current	349.1 (256–515)	92.1 (65–144)	441.2 (321–659)	3,036.5		3,477.8
Potential	623.5 (446–878)	172.1 (121–248)	795.5 (567–1,126)	3,176.4		3,971.9
Unrealized potential	274.4 (66–692)	80.0 (20–206)	354.4 (87–898)	139.8		494.2
Unrealized potential constrained	175.3 (38–453)	48.6 (11–131)	223.9 (49–584)	62.8		286.7
Unrealized potential adj. for 20, 30					225.0 (190.2–262.4)	
RCP8.5						
Potential	667.6 (643–690)	189.3 (181–197)	856.9 (825–887)			
Unrealized potential	318.4 (294–341)	97.2 (89–105)	415.6 (383–445)			
Unrealized potential constrained	202.6 (187–219)	60.3 (55–66)	262.9 (241–285)			
Erb et al. (19)						
Current			450 (380–536)			
Potential			916 (771–1,107)			
Unrealized potential			447 (272–702)*			
Bastin et al. (20, 30)						
Unrealized potential constrained					205.6 (133.2–276.2)	

Carbon pools include AGB, BGB, total biomass (AGB + BGB), SOC, and the sum of biomass and soil (AGB + BGB + SOC). Recent estimates from Erb et al. (19) and Bastin et al. (20, 30) are included for comparison. SOC$_b$ refers to the portion of SOC present in areas where woody biomass (i.e., AGB + BGB) is also present (e.g., SOC in grasslands is not included in SOC$_b$) and is included here to enable a more direct comparison with the results of Bastin et al. (20, 30) (see *SI Appendix,* Table S8 for further detail). Values are unconstrained (i.e., carbon stored in crop, grazing, and urban lands is included) except where indicated.
*Median and range of all 42 map combinations (7 current and 6 potential) from Fig. 1B of Erb et al. (19).

including crop and grazing lands, and human habitation (*SI Appendix,* Fig. S2). Approximately 27% (133.8 PgC) of the unconstrained pool was associated with croplands (18 PgC inclusive of shifting agriculture), 13% (64.9 PgC) was attributed to grazing lands, and another 2% (8.8 PgC) was associated with urban environments (SI Appendix, Table S1). Although some unrealized potential carbon could be reclaimed on agricultural lands via improved plant, animal, and/or nutrient management practices (6, 7, 22), to be conservative, we exclude agricultural lands from our estimates. In sum, the constraints reduced the unrealized potential carbon pool by 42%, leaving 286.7 PgC, with 223.9 PgC (49 to 584 PgC) available in biomass (a 37% reduction) and another 62.8 PgC available in soil (a 55% reduction) (Table 1). All subsequent mentions of "unrealized potential" carbon reference this constrained amount.

Of the three bioclimate zones (*SI Appendix,* Fig. S3), the tropical/subtropical zone (hereafter "tropics") holds, by far, the largest fraction of unrealized potential carbon (68%, 194.0 PgC; Fig. 2 and *SI Appendix,* Table S2). When considering biomass carbon alone, the tropics account for more than half (53%, 151.8 PgC) of the unrealized potential, 5 times more than the temperate zone (28.4 PgC) and nearly 3.5 times more than the boreal/polar zone (hereafter "boreal"; 43.8 PgC) (*SI Appendix,* Table S2).

The boreal and temperate zones hold approximately equal amounts (approximately 46 PgC) of unrealized potential carbon, with each accounting for around 50% of the extratropical total (92.8 PgC) (Fig. 2 and *SI Appendix,* Table S2). Yet, despite the apparent similarity in the additional storage opportunity offered by these zones, they differ significantly in the amount of unrealized potential distributed between biomass and soil pools. Whereas biomass represents about two-thirds

(62%; 28.4 PgC) of the unrealized potential in the temperate zone, it constitutes over 90% (43.8 PgC) of the opportunity in the boreal zone, where soil contributes just 2.9 PgC (*SI Appendix,* Table S2. While we report results for the boreal zone in the interest of completeness, unresolved questions about the net climate impact of biophysical feedbacks (e.g., albedo-induced warming; refs. 23, 24) and altered natural disturbance regimes (e.g., insect outbreaks and wildfire; ref. 25) on boreal ecosystems must be answered before the effective unrealized potential of the region can be determined.

NCS Opportunity. The NCS opportunity space includes seven broad categories for identifying the most relevant NCS action in a given location (Fig. 1). These spatially explicit and nonoverlapping categories were defined quantitatively using a data-driven approach based on thresholds of woody carbon density (see *Materials and Methods*). At the global scale, we find that over half (55%; 158.4 PgC) of the unrealized potential can be realized through maintenance and management (*MM*) of land with high suitability for forestry-based NCS (*H*) (Fig. 2 and *SI Appendix,* Table S3). When restoration (*R*) of land with high suitability for forestry-based NCS is also considered (22.7 PgC), the fraction increases to 63% (181.1 PgC). In contrast, *MM* and *R* of land with low suitability for forestry-based NCS (*L*)—principally open/low-density woody systems—account for just over one-fourth (27%; 78.7 PgC) of the available potential. Because our models do not explicitly account for the impact of natural disturbance regimes (e.g., frequent fires), estimates for these open/low-density woody systems should be viewed as upper bounds.

Not surprisingly, we find limited potential for additional carbon storage (7.9 PgC) in mature and largely undisturbed tracts
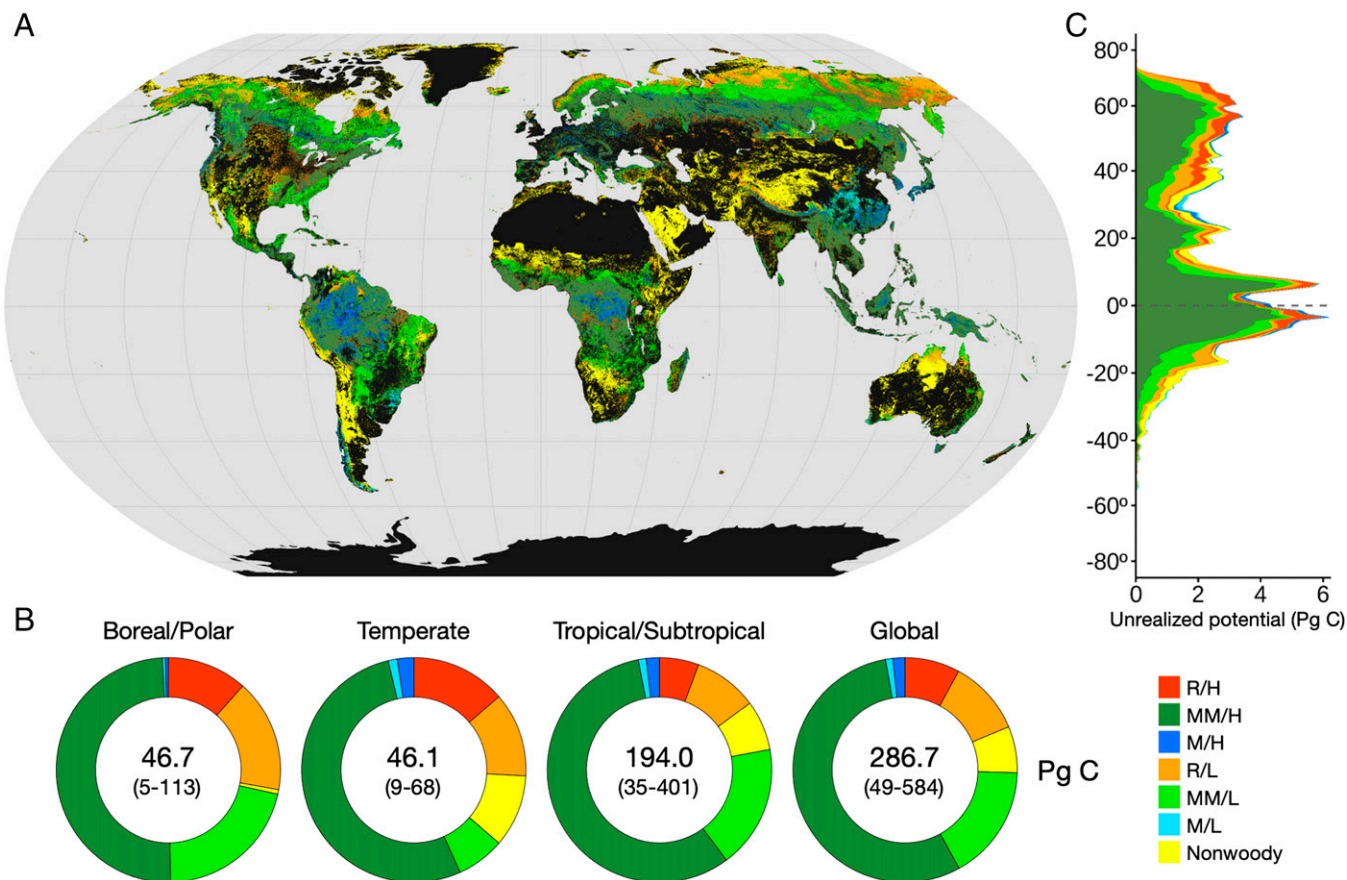
Fig. 2. The global distribution of NCS opportunities. (*A*) The geographic distribution of seven NCS opportunity categories. (*B*) The contribution of each opportunity category to unrealized potential carbon storage (PgC) among bioclimate zones and at the global scale. (*C*) The latitudinal distribution of unrealized potential carbon (PgC) storage in ABG, BGB, and SOC by opportunity category relative to *A*. Uncertainties reflect the AGB + BGB component only (see Table 1). All estimates are constrained to safeguard food production and human habitation.

of open and closed forest, defined here as being within 10% of their maximum storage capacity (see *Materials and Methods*). These landscapes represent less than 3% of the global unrealized potential; however, they also account for nearly one-fifth (18%, 79.4 PgC) of the carbon currently stored in woody biomass across more than 500 million hectares of forest globally (*SI Appendix,* Tables S3 and S4). It follows that *M* of this largely intact carbon pool (i.e., avoiding emissions from conversion or degradation) represents the primary NCS intervention relevant to this category.

Among the three bioclimate zones, we find that *MM* of tropical ecosystems characterized as highly suitable for forestry-based NCS (*MM/H*: 110.9 PgC) affords the single largest NCS opportunity, more than twice the potential of the *MM/H* opportunity offered by the boreal and temperate zones combined (47.5 PgC) and nearly 40% of the global potential (Fig. 2 and *SI Appendix,* Table S3). Tropical biomass alone (99.1 PgC) accounts for nearly 90% of the potential offered by *MM/H* across the tropics. The tropics also claim the second largest opportunity category, with *MM/L* accounting for another 18% (34.5 PgC) of the zone's unrealized potential (194.0 PgC) or 12% of the global total (286.7 PgC; *SI Appendix,* Table S3). However, the effective opportunity afforded by this category necessarily requires further research into the potential impacts of natural disturbance regimes.

Restoration (*H* + *L*) accounts for 28% (13 PgC), 26% (11.9 PgC), and 15% (28.9 PgC) of the unrealized potential in the boreal, temperate, and tropical zones, respectively. While the tropics have as much restoration potential as the other two zones combined (Fig. 2 and *SI Appendix,* Table S3), maintenance and

management (*MM* + *M*) of all tropical systems (151.3 PgC) offers over 5 times more potential for additional land-based carbon storage than *R* of tropical woody carbon stocks (*H* + *L*) (28.9 PgC). This analysis considers the potential for land carbon restoration only in places where woody biomass is naturally dominant, excluding nonwoody systems (e.g., grasslands) where woody biomass additions can have negative consequences for biodiversity and ecosystem health. Nevertheless, nonwoody systems do offer modest opportunities for additional carbon storage in both temperate (4.8 PgC) and tropical (14.0 PgC) zones, with soil carbon necessarily accounting for nearly 90% (16.6 PgC) of the available opportunity (*SI Appendix,* Table S3).

At the national level, the top 25 contributors to the unrealized potential for additional land carbon storage account for nearly three-fourths (74%; 213 PgC) of the global total (Fig. 3*A* and *SI Appendix,* Table S5). Of these countries, the top seven—Russia, Brazil, United States, China, Democratic Republic of the Congo (DRC), Indonesia, and Canada—represent fully 50% (141.9 PgC) of the available sum. Russia alone accounts for 15% (42.0 PgC) of the global total, with the four *R* and *MM* opportunity categories contributing at least 5 PgC each (*SI Appendix,* Table S6). However, more than 80% (33.8 PgC) of Russia's unrealized potential carbon is within the boreal zone (*SI Appendix,* Table S6), and uncertainties about the effects of albedo and other nongreenhouse gas factors means more research is needed before the true value of Russia's climate mitigation opportunity can be quantified. Removing the boreal component (33.8 PgC) of Russia's total unrealized potential (42.0 PgC) leaves the country with just 8.2 PgC, dropping it to

eighth place in the top 25 list (*SI Appendix*, Table S5). Similarly, removing the boreal contribution (approximately 70%; 7.2 PgC) from Canada's seventh place total (10.4 PgC) drops it to 18th place (3.2 PgC), tied with Papua New Guinea.

Ranking countries in terms of their absolute unrealized potential necessarily overlooks the per-unit-area potential of their NCS opportunity (hereafter, "opportunity density"). When we consider the opportunity density of the top 25 countries (Fig. 3*B*), we observe a significant rank reordering, with the Philippines, Indonesia, Myanmar, Madagascar, and Tanzania comprising the top five despite ranking no higher than sixth (i.e., Indonesia) in absolute terms (Fig. 3*A*). Notably, the Philippines, Madagascar, and Tanzania moved from the bottom five in terms of absolute unrealized potential (ranging from 2.5 to 2.8 PgC) (Fig. 3*A*) to the top five in terms of opportunity density (ranging from 74 to 123 MgC ha^{-1}) (Fig. 3*B*), with the Philippines climbing from 25th place to a ranking of first when the area of its opportunity is considered. In contrast, Indonesia maintains a high position in both rankings: sixth in terms of absolute potential (12 PgC) (Fig. 3*A*) and second in terms of opportunity density (84 MgC ha^{-1}) (Fig. 3*B*). Perhaps unsurprisingly, the largest countries—including Russia and China, which rank among the top five in absolute terms—drop to the bottom five when accounting for the significant land area across which the opportunity for additional carbon storage is distributed.

Of the seven NCS opportunity categories, *MM/H* is, by far, the largest contributor to the unrealized potential among the top 25 countries. Not only does *MM/H* account for more than 40% (117.7 PgC) of the global total (*SI Appendix*, Table S5), but the opportunity exhibits a wide geographic distribution, with 21 of the top 25 countries—and 29 countries in total— each having the potential to realize at least 1.5 PgC (0.5% of the global total) through *MM/H* activities. The opportunity is concentrated in Africa and Asia, where the Philippines, Madagascar, Nigeria, Indonesia, and Ethiopia comprise the top five in terms of opportunity density (Fig. 3*E*). In comparison, the second largest contributor, *MM/L*, represents 13% (35.9 PgC) of the total unrealized potential, with eight countries meeting the 1.5-PgC threshold (*SI Appendix*, Table S5) and the highest concentrations observed in the Philippines and Nigeria (Fig. 3*F*).

The *R* of woody biomass (*H + L*) across the top 25 countries offers 41.9 PgC of additional land carbon storage (approximately 15% of the global total) and at least 1.5 PgC of NCS opportunity in seven countries: Russia, Brazil, United States, China, Canada, Australia, and India (*SI Appendix*, Table S5). The *R* opportunity afforded by these countries (30.7 PgC) is shared between landscapes characterized by both high (12 PgC) and low (18.7 PgC) suitability for forestry-based NCS, though we note that restoration in the latter landscapes must be carefully implemented to avoid pushing these systems past their natural carrying capacity for carbon. An additional 11 countries (DRC, Mexico, Angola, Peru, Colombia, Nigeria, Bolivia, Venezuela, Tanzania, Madagascar, and Ethiopia) each offer 0.5 to 1.5 PgC (7 PgC total) of *R* opportunity between *H* and *L* systems (*SI Appendix*, Table S5). In sum, the 18 countries offering modest (0.5 to 1.5 PgC) to potentially significant (≥1.5 PgC) woody-carbon restoration potential (*H + L*) account for 70% (37.7 PgC) of the global *R* opportunity and 13% of the global total (*SI Appendix*, Table S5). Of this list, Colombia, DRC, and Indonesia all exhibit densities of unrealized potential carbon >80 MgC ha^{-1}, placing them among the top five countries in terms of the opportunity density offered by *R* (Fig. 3 *C* and *D*).

Not surprisingly, we find the top 25 countries in the *M* category (*H + L*) hold relatively limited potential for additional land carbon storage (6.1 PgC), which necessarily consists of mature, largely intact forests and other woody-dominated systems (*SI Appendix*, Table S5). The greatest opportunity for additional carbon storage is observed in China and Brazil (3.5 PgC), with the remainder (2.6 PgC) spread across 13 countries having the potential to contribute at least 0.1 PgC each. Nevertheless, the mature forests in these countries already store considerable carbon in woody biomass (68.4 PgC) and soil (177.6 PgC) (*SI Appendix*, Table S7), highlighting the importance of *M* of at-risk high-carbon systems.

Projected Climate-Driven Risk by 2050. Climate change—specifically, changes in temperature and precipitation—is a large source of uncertainty where the opportunity for additional carbon storage on land is concerned (Fig. 4). Our analysis of the differential influence of climate change on ecosystem carbon stocks, which assumes RCP8.5 to be the best predictor of future climate out to 2050 (26), reveals a projected average increase of 17% (8 to 27%) in the unrealized potential for additional land carbon storage in global biomass (AGB + BGB; Table 1). This overall increase of 39 PgC, which does not account for climate change feedbacks and associated changes in plant physiology or natural disturbance regimes, belies considerable variability among the three bioclimate zones. Whereas the boreal and temperate zones are projected to increase by 114% (78 to 151%) and 25% (16 to 30%), respectively, the tropics are projected to decrease by 12% (7 to 16%) (Fig. 4*B* and *SI Appendix*, Table S2). In absolute terms, this translates to projected increases of ~50 PgC (34 to 66 PgC) and 7 PgC (5 to 9 PgC) in the boreal and temperate zones, respectively. This contrasts with the tropics, where climate change is projected to reduce the unrealized potential of 152 PgC by some 18 PgC (11 to 24 PgC). Nevertheless, the tropics are anticipated to experience the smallest shift in the density of unrealized potential carbon storage in biomass, losing just 5 MgC ha^{-1} on average, as compared to nearly 7 MgC ha^{-1} of loss and almost 26 MgC ha^{-1} of gain on average in the temperate and boreal zones, respectively (Fig. 4*C* and *SI Appendix*, Table S3).

Among the six primary NCS opportunity categories, only lands in the *MM/H* category are projected to suffer a substantial net decline (approximately 17 PgC; 12%) in the potential to store additional carbon in biomass by 2050, with the entirety of the gross decrease (34.3 PgC) projected to occur within the tropics (Fig. 4*D* and *SI Appendix*, Table S3). The remaining NCS opportunity categories are predicted to exhibit either relative stability or gains in potential carbon storage under RCP8.5, with the largest projected increases associated with the *M* of mature and largely undisturbed tracts of open (*L*) (1,500%; approximately 5 PgC) and closed (*H*) (119%; approximately 3 PgC) forest. However, because much of this projected increase (62%; approximately 5 PgC) can be attributed to the boreal zone, where the effects of intensifying fire regimes and changes in albedo on ecosystem carbon dynamics remain uncertain (27), accounting for these impacts would likely reduce the net climate benefit reported here (Fig. 4*D* and *SI Appendix*, Table S3).

Our data also support national and subnational assessments of the risk to climate-induced changes in the potential for additional carbon storage in biomass (Fig. 4*A*). For example, Brazil, which represents more than 10% of the global biomass opportunity, is projected to experience a decline in unrealized potential biomass carbon storage on the order of 22% (9 to 26%) for an average reduction of approximately 5 PgC (2 to 6 PgC; AGB + BGB) (Fig. 5*A*). Where specific NCS opportunities in Brazil are concerned, we project the largest declines in the *R/H* (19%) and *MM/H* (60%) categories, where a total reduction in potential of
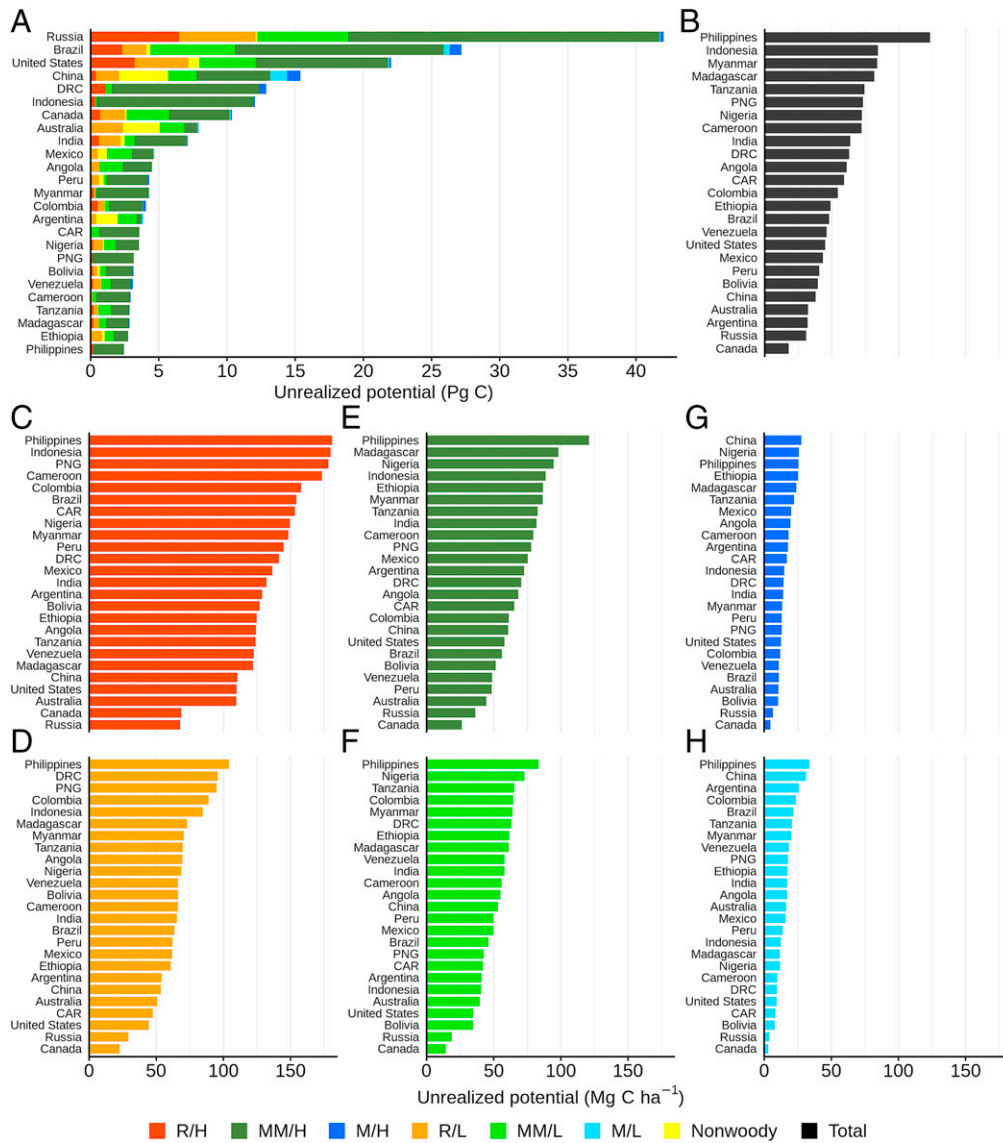
Fig. 3. Top 25 countries ranked in terms of total constrained unrealized potential carbon stored in biomass and soil. (*A*) The total opportunity by country across seven NCS opportunity categories, which accounts for almost 75% of the total constrained unrealized potential for additional land carbon (PgC) storage. (*B*) The total by country in *A* expressed per unit area of opportunity (i.e., opportunity density). (*C–H*) The opportunity density by country in *A* disaggregated among six opportunity categories: R/H, MM/H, M/H, R/L, MM/L, and M/L.

9 PgC is predicted. Conversely, sizeable gains are predicted across all categories of land with *L*, including *R/L* (43%), *MM/L* (61%), and *M/L* (2900%). In absolute terms, however, these relative gains are small in comparison to the losses projected for land with *H*. However, carbon stocks in these systems are often maintained at lower levels by natural disturbance, which may increase under future climate; thus, these projected gains are best viewed as upper bounds. Regardless, these results confirm the importance of considering the impact of climate-induced changes on potential carbon storage as part of national and subnational efforts to prioritize and implement forestry-based NCS.

Discussion

Our results strengthen the growing body of research devoted to quantifying the potential for NCS to mitigate climate change by providing critical limits on the potential for land-based carbon storage and elucidating the most relevant actions for storing additional carbon. While reducing fossil fuel emissions is of paramount importance, increasing carbon storage in land-based

reservoirs provides a significant opportunity to remove additional carbon from the atmosphere. We estimate an untapped global land carbon reservoir of approximately 286.7 PgC after safeguarding areas critical to food production and human habitation (Table 1). Discounting storage opportunities offered by the restoration of woody biomass in boreal (*R/H*) (12.6 PgC; given potential albedo decreases), tropical transitional (*R/L*) (13.6 PgC; given potential biodiversity impacts), and nonwoody/grassland (2.4 PgC; given potential biodiversity impacts) systems, the potential for additional land carbon storage globally is 258 PgC. Approximately 70% (178 PgC) of this remaining unrealized potential is found in the tropics, where a single NCS opportunity category—the maintenance and improved management of degraded forests (*MM*) (145.4 PgC)—represents a significant yet underappreciated opportunity, offering 5 times the mitigation potential of tropical forest restoration (28.9 PgC) and over 3.5 times the potential of temperate and tropical forest restoration (40.8 PgC) combined (*SI Appendix*, Table S3). Climate change impacts could diminish the magnitude of this *MM* opportunity by as much as 38% by 2050, with further reductions possible due to changes in human and/or
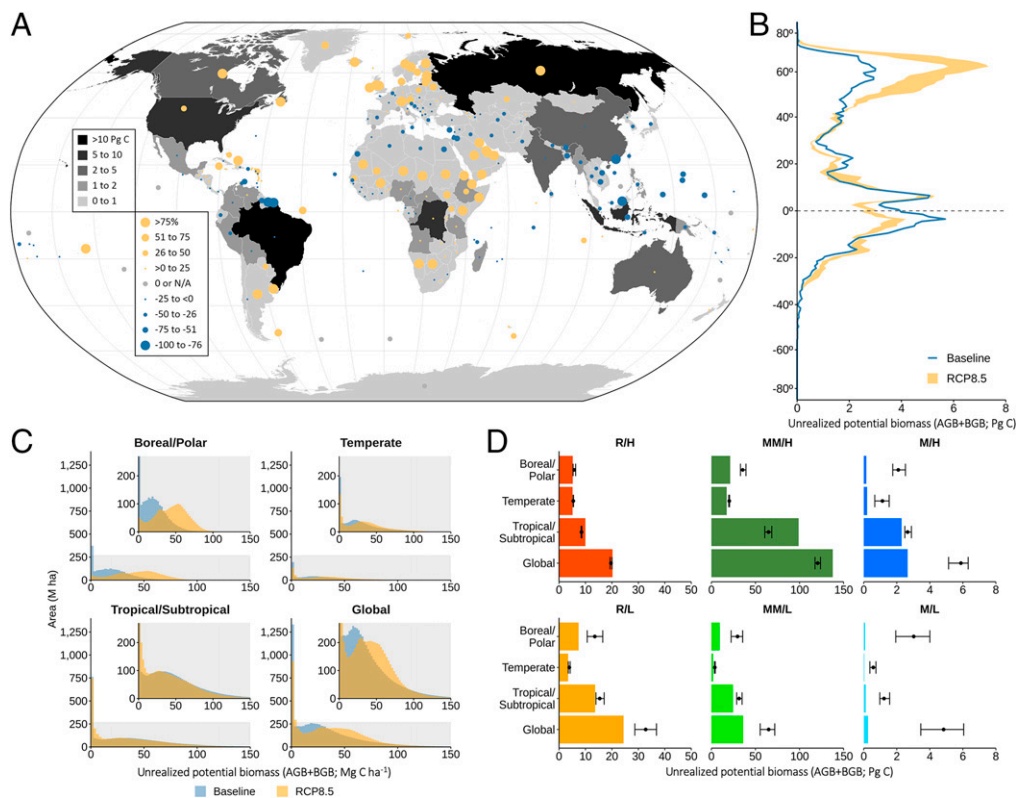
Fig. 4. Projected risk of change in the unrealized potential carbon stored in ABG + BGB by 2050 due to climate change (RCP8.5). (*A*) Country-level map illustrating baseline (1960 to 1990) unrealized potential carbon storage (PgC) and change (%) relative to RCP8.5 (mean of 11 Earth system models). (*B*) Latitudinal distributions of unrealized potential carbon storage (PgC) assuming baseline climate (blue line) and future climate (yellow envelope; RCP8.5; range of 11 Earth system models). (*C*) Distribution of unrealized potential carbon density (MgC ha^{-1}) by bioclimate zone under baseline and future climate (RCP8.5; mean of 11 Earth system models). Insets truncate the *y*-axis range to 270 Mha. (*D*) Total unrealized potential carbon (PgC) storage by bioclimate zone and NCS opportunity category under current climate (colored horizontal bars) and future climate (black symbols representing RCP8.5; mean and range of 11 Earth system models). All estimates are constrained to safeguard food production and human habitation.

natural disturbance regimes (e.g., increasing deforestation/degradation and/or fire frequency/intensity), reinforcing the need for rigorous data-driven planning and prioritization informed by expert knowledge of conditions on the ground (28).

Our study employs a direct approach to estimating current and potential carbon storage that avoids the uncertainty associated with multistep, area-based assessments (29), which differ widely in terms of both ends (results) and means (methods) and have fueled much debate, particularly about the absolute mitigation potential afforded by tree-planting initiatives and broader forest restoration activities (30, 31). Nevertheless, when we compare our results with recent empirical analyses on equal carbon-based terms, while accounting for differences in definitions and methods, we observe broad agreement. Bastin et al. (20, 30), in their area-based study of global tree restoration potential, reported an additional land carbon storage capacity of 205.6 PgC, ranging from 133.2 to 276.2 PgC (Table 1). Following a reanalysis of our data to replicate, in so far as possible, the methods and constraints employed by Bastin et al. (20)—including 1) a narrower geographic focus (limited to lands capable of supporting additional canopy cover; i.e., tree restoration) 2) less conservative societal constraints (crop and urban areas removed but not grazing lands), and 3) a shallower soil depth (1 m vs. 2 m) compared to this study (*SI Appendix,* Table S8)—we found 225.0 PgC (190.2 to 262.4 PgC) of unrealized potential, a value within 10% of the mid-range estimate (205.6 PgC) of Bastin et al. (30) and well within their reported range (133.2 to 276.2 PgC).

In another recent analysis, Erb et al. (19) reported unconstrained global estimates of current (450 PgC; 380 to 536 PgC),

potential (916 PgC; 771 to 1,107 PgC), and unrealized potential (447 PgC; 272 to 702 PgC) carbon storage in plant biomass (AGB + BGB) following a statistical aggregation of several disparate map-based estimates (Table 1). Erb et al. (19) did not apply societal constraints in their analysis, precluding a direct comparison of their findings with Bastin et al. (20, 30); however, we find that our unconstrained estimate of current carbon storage in woody biomass (441.2 PgC; 321 to 659 PgC) agrees closely with their calculated mean (450 PgC), and our analogous estimate of potential carbon storage (795.5 PgC; 567 to 1,126) falls within their reported range (771 to 1,107 PgC), albeit near the lower bound. Our unconstrained estimate of unrealized potential carbon storage (354.4 PgC; 87 to 898 PgC) is also well within their range (272 to 702 PgC), falling just below the minimum of their inner quartiles (375 to 525 PgC) (Table 1).

Several earlier studies provide historical reconstructions of net carbon emissions from land-use and land-cover change using process- or bookkeeping-based modeling approaches. While preindustrial (pre-1850) estimates vary considerably, ranging from as high as 325 to 357 PgC (18) to as little as 48 to 153 PgC (11, 12, 15), postindustrial (post-1850) estimates tend to be lower and better constrained, ranging from 108 to 188 PgC, including both biomass (AGB and BGB) and soil organic matter (11–17). Subtracting the reported postindustrial range (108 to 188 PgC) from our unconstrained estimate of unrealized potential carbon storage in woody biomass and soil (494.2 PgC) yields a balance of 306.2 to 386.2 PgC. The midpoint of this range (346.2 PgC) agrees closely with the midpoint (341 PgC) of the upper bounding range (325 to 357 PgC) proposed by Kaplan et al. (18), who assume nonlinear
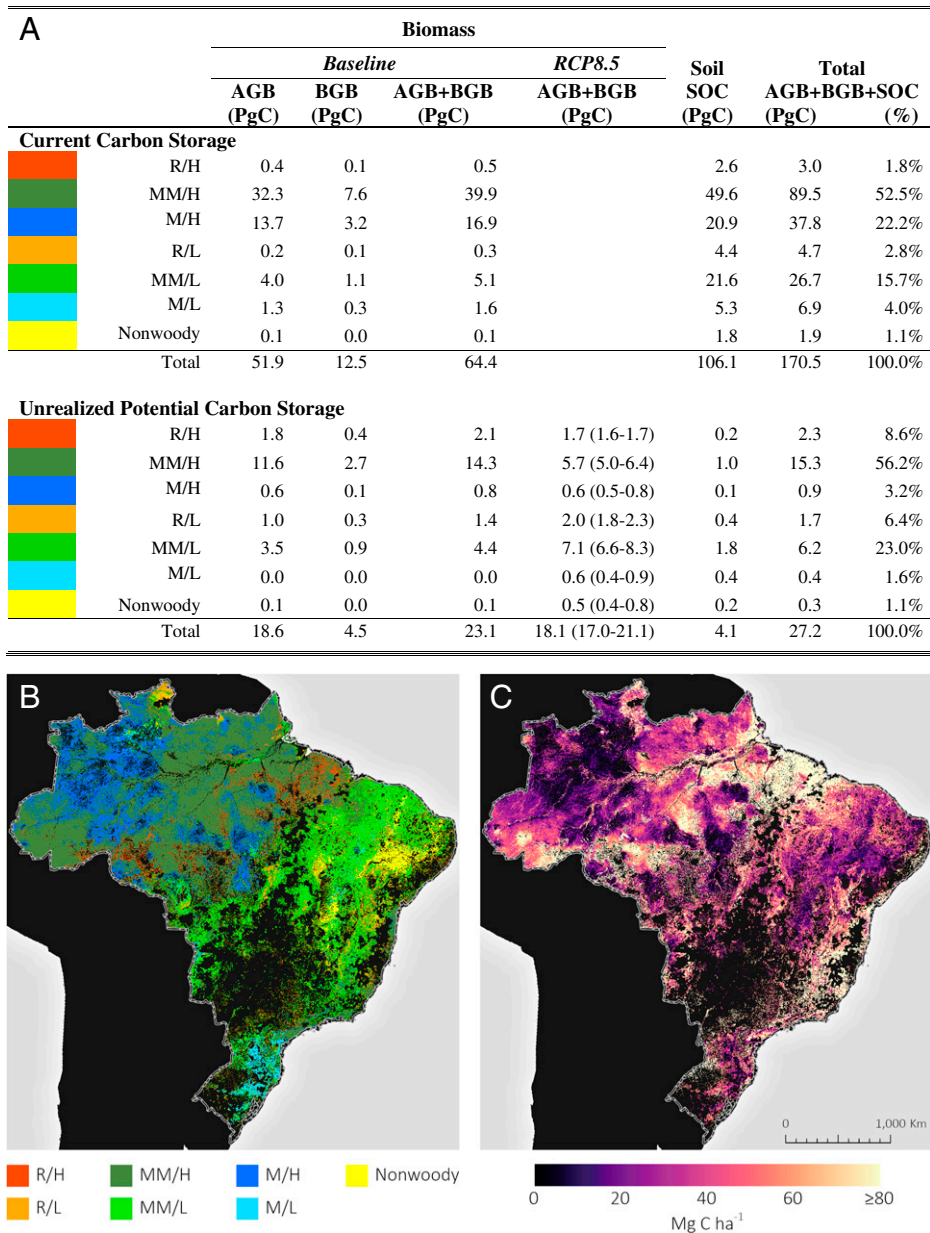
A

	Biomass				Soil	Total	
	Baseline			RCP8.5	SOC	AGB+BGB+SOC	
	AGB (PgC)	BGB (PgC)	AGB+BGB (PgC)	AGB+BGB (PgC)	SOC (PgC)	(PgC)	(%)
Current Carbon Storage							
R/H	0.4	0.1	0.5		2.6	3.0	1.8%
MM/H	32.3	7.6	39.9		49.6	89.5	52.5%
M/H	13.7	3.2	16.9		20.9	37.8	22.2%
R/L	0.2	0.1	0.3		4.4	4.7	2.8%
MM/L	4.0	1.1	5.1		21.6	26.7	15.7%
M/L	1.3	0.3	1.6		5.3	6.9	4.0%
Nonwoody	0.1	0.0	0.1		1.8	1.9	1.1%
Total	51.9	12.5	64.4		106.1	170.5	100.0%
Unrealized Potential Carbon Storage							
R/H	1.8	0.4	2.1	1.7 (1.6-1.7)	0.2	2.3	8.6%
MM/H	11.6	2.7	14.3	5.7 (5.0-6.4)	1.0	15.3	56.2%
M/H	0.6	0.1	0.8	0.6 (0.5-0.8)	0.1	0.9	3.2%
R/L	1.0	0.3	1.4	2.0 (1.8-2.3)	0.4	1.7	6.4%
MM/L	3.5	0.9	4.4	7.1 (6.6-8.3)	1.8	6.2	23.0%
M/L	0.0	0.0	0.0	0.6 (0.4-0.9)	0.4	0.4	1.6%
Nonwoody	0.1	0.0	0.1	0.5 (0.4-0.8)	0.2	0.3	1.1%
Total	18.6	4.5	23.1	18.1 (17.0-21.1)	4.1	27.2	100.0%

Legend: R/H, MM/H, M/H, Nonwoody, R/L, MM/L, M/L

Color scale (C): 0, 20, 40, 60, ≥80 Mg C ha^{-1}

Scale bar: 0 — 1,000 Km

Fig. 5. The opportunity for additional carbon storage in Brazil. (*A*) Carbon (PgC) stored in current and unrealized potential AGB, BGB, total biomass (AGB + BGB), SOC, and the sum of biomass and soil (AGB + BGB + SOC) in Brazil by NCS opportunity category. Estimates of unrealized potential carbon storage in total biomass (ABG + BGB) by 2050 due to climate change (RCP8.5; mean and range of 11 Earth system models) are also included. Maps depict the geographic distribution of (*B*) seven NCS opportunity categories and (*C*) unrealized potential carbon (MgC ha^{-1}) storage (assumes baseline climate). All estimates are constrained to safeguard food production and human habitation.

(i.e., decreasing) rather than constant rates of per-capita land use over the last ca. 7,000 y (18, 32). Thus, our results support the higher estimates of preindustrial carbon losses from land-use change.

These literature-based comparisons, taken together with our own model performance (*SI Appendix,* Figs. S4–S7) and validation analyses (*SI Appendix,* Figs. S9 and S10 and Table S8), suggest that our unconstrained estimate of unrealized potential carbon storage (494.2 PgC) may be conservative. Intact forests (i.e., absent human-induced degradation) are an increasingly rare feature globally, comprising as little as 18% of the planet's remaining forest area (33), which means many regions lack examples of mature/old growth forest that are at or near their maximum carbon storage capacity. This translates to a lack of calibration data across the full range of potential woody biomass densities needed to accurately model potential carbon storage across all ecoregions. Although the geographic extent and magnitude of this underprediction are unclear (*SI Appendix,* Figs. S4 and S5) and will be offset in some geographies by reductions associated with altered natural disturbance regimes and biophysical feedbacks, they are factors to be considered in the interpretation of the results in regions where historical impacts of human settlement on current carbon density are pronounced (e.g., the northeastern United States and western Europe).

Our approach, which provides a top-down spatially explicit global estimate of potential additional carbon storage, is not directly comparable with bottom-up studies that estimate the annual climate mitigation potential derived from discrete NCS actions to improve land stewardship (e.g., refs. 4, 9). The climate benefits resulting from bottom-up analyses of disaggregated, time-bound interventions (e.g., forest restoration or improved forest management activities) are not intended to be

summed over long periods as a means of estimating the total unrealized climate mitigation potential of land-based NCS. These studies are designed for near-term (e.g., midcentury) outlooks. Declines in sequestration rates as forest stands approach maturity are regionally variable and poorly understood compared to the sequestration rates of younger stands (34). Nevertheless, reconciling bottom-up and top-down analyses is central to the planning and implementation of long-term climate policy ambitions. The top-down spatially explicit identification of areas that have high rates of carbon accumulation and high capacities for additional carbon storage helps to more efficiently target bottom-up analyses to determine which NCS interventions are best suited to a given location.

Differences in methods complicate comparisons of our top-down analysis with bottom-up studies; however, we look at proportional (rather than absolute) comparisons to understand notable areas of agreement and disagreement. For example, we find that over two-thirds (68%; 194.0 PgC) of unrealized potential carbon storage is found in the global tropics (*SI Appendix,* Table S2). This result is only slightly higher than the bottom-up mitigation potential (based on annual change in CO_2e fluxes) available through analogous NCS actions in the tropics (61%) as reported by Griscom et al. (6), who applied similar food security and human settlement safeguards. Together, these results reinforce the conclusion that NCS represent important opportunities for tropical countries.

While our spatially explicit approach does not provide bottom-up estimates of enhanced land carbon storage available through specific NCS pathways (e.g., as reported by refs. 4, 9) (see *SI Appendix,* Table S9 for a summary of NCS pathways relevant to each opportunity category), it does provide a practical spatial framework that can be used in NCS planning efforts, specifically in determining which NCS opportunity categories offer the largest climate benefit. Applying this framework to Brazil, for example, reveals that over half (53%; 14.3 PgC) of its capacity for additional land carbon storage (27.2 PgC) can be achieved through the *MM* of woody biomass, primarily in the Amazon region, where there is high suitability for forestry-based NCS (*H*) (Fig. 5). When land with low suitability for forestry-based NCS (*MM/L*)—primarily located in the Cerrado and Caatinga regions—is also considered (4.4 PgC), the combined contribution of *MM* of woody biomass to Brazil's capacity for additional land carbon storage approaches 70%; the inclusion of soil (2.8 PgC) increases the contribution to nearly 80% (Fig. 5*A*). Climate change could reduce the potential of the *MM* opportunity in woody biomass by more than 30% by 2050, making clear that while the climate crisis demands that NCS be implemented now, the projected impacts of climate change on the fundamental characteristics of the NCS opportunity space must factor prominently in the process of planning and prioritization (28).

Perhaps counterintuitively, restoration (*R*) of land with high suitability for forestry-based NCS (*H*) affords less than 10% of Brazil's untapped climate benefit. Although the country's history of extensive forest loss is well documented (35), our decision to safeguard (i.e., remove from consideration) areas critical to ongoing food production and human habitation means reforestation has a limited role to play, and the greatest gains are to be achieved by focusing conservation restoration and improved forest management efforts on areas where forest cover has been at least partially maintained and/or restored. Given recent increases in rates of deforestation across Brazil (36, 37), maintenance of current carbon stored in woody biomass (64.4 PgC) and soil (106.1 PgC)—regardless of opportunity category—should be prioritized.

Our carbon-based framework for conceptualizing the NCS opportunity space (Fig. 1) and its utility for prioritizing on-the-ground action has important advantages over alternative approaches. First, the emphasis on continuous, spatially explicit estimates of carbon density avoids much of the uncertainty associated with methods based on tree cover or forest area and derivative approximations of potential land carbon storage. Second, the framework is intended to be flexible and nonprescriptive. For example, the carbon-based thresholds we apply at the scale of bioclimate zones are neither hard-and-fast nor normative; rather, they reflect both opportunities and risks involved in identifying NCS across the restore–manage–maintain spectrum and can be adjusted or redefined to better reflect national or subnational circumstances and priorities. Decisions about which solutions are preferred must be informed by and aligned with local realities, including more refined accounting of carbon and other ecosystem services, biodiversity, and social justice. Third, while climate change is a source of considerable uncertainty that will assuredly impact the magnitude and spatial distribution of NCS opportunities moving forward, our data inform how maximum carbon storage could shift in response to changing environmental conditions. Finally, while our framework includes all major carbon pools and global geographies, making it well suited to landscape-level prioritization among broad categories of NCS action, we demonstrate its utility rather than prescribe any given action in any particular location. The completeness affords users a "menu of options" from which to choose specific interventions and regions of focus, while geographies of special concern can be excluded from consideration in response to expert knowledge of local conditions, including projected human and natural disturbances. For example, we distinguish woody-dominated transitional systems with low suitability for forestry-based NCS (Fig. 1), which might be regionally or locally defined as savanna or woodland ecosystems. Our approach should not be interpreted to mean management of these globally important systems toward "forests" as traditionally defined by tree cover, but rather management toward the mature (i.e., potential) woody carbon density characteristics and associated biodiversity complement of the native ecosystems.

While we include spatially explicit constraints to address areas critical to food production, human habitation, and sensitive biodiversity, there is a wider set of constraints and opportunities that future studies should consider. These considerations should include technical, economic, socio-political, and governance constraints as well as climate feedbacks, associated biophysical effects (e.g., local to regional changes in wildfire regimes and albedo), and ecosystem service opportunities (38, 39). While many of these constraints and opportunities have been disaggregated to national scales (39), further research is needed to resolve their spatial distribution at scales relevant to on-the-ground management.

In particular, more work is needed to better constrain the potential uncertainty that climate change is likely to impose on the NCS opportunity space. In our analysis, where historical precipitation- and temperature-based climate indicators are replaced with ca. 2050 (RCP8.5) analogs to estimate future carbon storage potential, we address only the radiative effects of climate change (i.e., our generalized predictive model does not allow for coupled dynamics and, thus, excludes climate change feedbacks and physiological effects, including CO_2 fertilization—the estimates of which are poorly constrained, highly variable, and contingent on the methods employed) (40–42). While there is strong evidence that a greening of the terrestrial biosphere has occurred during the satellite era, this trend is not driven by CO_2 fertilization, apart from in cool grasslands and temperate forests, and has weakened since 2000 (41). Several browning hotspots are

now emerging, especially in the tropics. This browning, a decline in photosynthetic capacity and therefore carbon uptake, is consistent with current trends of land carbon sink saturation (43) or degradation (44) as well as the temperature dependence of global photosynthesis and respiration—and, thus, carbon storage—under realized and anticipated warming (45). In addition, episodes of forest mortality linked to drought and wildfire under climate change (28, 46) cannot be captured with WorldClim 1.4 bioclimatic data. On balance, then, while the influence of these missing factors on future carbon storage potential remains uncertain, we hypothesize their exclusion results in an optimistic assessment (i.e., our estimate is best viewed as an upper bound on the available reservoir). But regardless of the reservoir's ultimate magnitude, it is important to also acknowledge that the asymmetric response of the climate system to CO_2 emissions and removals means that any attempt to offset an emission with an equivalent removal will lead to a higher atmospheric concentration than if the emission had been altogether avoided (47, 48). It follows that maintenance and improved management of existing carbon stocks should be prioritized over restoration efforts whenever possible (49).

Our results point to an emerging consensus about the magnitude and spatial distribution of the land carbon reservoir available to support NCS actions globally. Through comprehensive improvements on previous research, including advances in spatial resolution (approximately 500 m) and biophysical completeness (e.g., AGB, BGB, and soil) and development of a conceptual framework for defining an NCS opportunity space, while also safeguarding critical geographies and considering future climate impacts, we provide an absolute reference point, a spatially explicit framework, and a practical tool for guiding decision-makers in identifying the upper bound for NCS to deliver climate benefit.

Materials and Methods

The following sections describe the development of spatially explicit estimates of 1) current carbon storage (ca. 2016), 2) potential carbon storage (under baseline and RCP8.5 climates), and 3) unrealized potential carbon storage in AGB (i.e., leaves, branches, and stems), BGB (i.e., roots), and soil (i.e., organic carbon) (*SI Appendix*, Fig. S1). When possible, we produce separate pool-specific data products to facilitate comparisons of the relative magnitude of the various carbon pools within a given geography (e.g., region or country) as well as with other studies that examine only a subset of pools.

Aboveground Carbon Storage.
Current aboveground carbon. Our spatially explicit global estimate *of current carbon density* (ca. 2016) in AGB is based on published methods developed by Baccini et al. to produce pantropical-scale (21, 50–52) and global-scale (53, 54) maps of AGB stock and change. The mapping approach combines field measurements with colocated airborne and spaceborne (NASA ICESat Geoscience Laser Altimeter System; GLAS) lidar data to yield a global pseudoinventory of 53.9 million spatially explicit estimates of AGB density at the GLAS footprint (∼60-m diameter) scale (52) (*SI Appendix*, Table S10). Tree-based regression models relating GLAS-based estimates of AGB to wall-to-wall satellite imagery acquired (ca. 2016) by the Moderate Resolution Imaging Spectroradiometer (MODIS) are then used to generate a spatially explicit snapshot of global AGB density (Mg ha^{-1}; ca. 2016) at a resolution of approximately 500 m (i.e., 463 m; 12.4 ha).

The generalized predictive model takes the form of

$$AGB_C = f(CL, S, T, R) \qquad [1]$$

where AGB_C (current AGB) is a function of predictor variable classes. *CL*, climate variables; *S*, soil variables; *T*, topographic variables (i.e., elevation and slope); *R*, reflectance information derived from multispectral satellite data. A total of 194 tiled (10° × 10°) predictors were used: 67 WorldClim 1.4 climate variables reflecting baseline climate (ca. 1960 to 1990 average) conditions (55), 59 SoilGrids soil variables (56), 2 topographic variables (57, 58), and 66 MODIS spectral reflectance variables (*SI Appendix*, Table S11). Separate random forest models were developed for each of six ecoregional realms (*SI Appendix*, Fig. S11):

Australia, Afrotropic, Nearctic, Neotropic, Palearctic, and Tropical Asia (59). Prior to model calibration, 20% of the pixels in each realm were withheld for accuracy assessment. Additional methods details as well as an assessment of model performance can be found in *SI Appendix*.

Potential aboveground carbon (baseline 1960 to 1990). *Modeling approach.* The approach to generating the ca. 2016 global map of current carbon density in woody AGB provided the basis for developing a second global data product: a map of potential carbon density in woody AGB, defined here as the maximum accumulation of carbon that can be realized anywhere on the landscape assuming current (i.e., baseline) biogeophysical conditions and the absence of human disturbance. Achieving interproduct consistency and comparability in the current and potential datasets was central to the overall mapping strategy, and with few key exceptions, the approaches to generating the two products mirror one another. The key difference lies in the form of the generalized predictive model:

$$AGB_P = f(CL, S, T) \qquad [2]$$

where AGB_P (potential AGB) is a function of predictor variable classes. *CL*, climate variables; *S*, soil variables; *T*, topographic variables (i.e., elevation and slope). The sole difference between Eqs. 2 and **1**, the latter of which specifies the model for predicting AGB_C, is that [2] does not include reflectance data derived from contemporary satellite imagery (i.e., MODIS). As such, AGB_P can vary only as a function of biophysical variables, meaning the primary drivers of AGB accumulation in this model are current climatic, edaphic, and topographic factors. As such, human disturbance, and its associated influences on the geographic amount and distribution of AGB, is effectively removed from the model. A total of 186 tiled (10° × 10°) predictors were used: 67 WorldClim 1.4 climate variables reflecting baseline climatic (ca. 1960 to 1990 average) conditions (55), 117 SoilGrids soil variables (56), and 2 topographic variables (57, 58) (*SI Appendix*, Table S11).

The global pseudoinventory of GLAS-based estimates of AGB was again used for model calibration and validation; however, the 53.9 million available samples were first filtered to provide, to the extent possible, an accurate representation of potential rather than current global AGB. Filters were applied to remove GLAS shots located 1) within 2 km of any road (60); 2) within 500 m of forest gain or loss between 2000 and 2012 as defined by Hansen et al. (61); or 3) within the Urban and built-up, Cropland, or Cropland/Natural Vegetation Mosaic classes of the International Geosphere-Biosphere Programme's land cover product (62). The Center for International Earth Science Information Network's gROADSv1 dataset (60) was the source for all road data except for northeastern Pakistan, where Digital Chart of the World data (63) were used to fill missing data. The exception to this filtering scheme concerned GLAS shots falling within the 2013 Intact Forest Landscapes (IFL) layer of Potapov et al. (64). This subset of GLAS shots was included in the final calibration data set in its entirety as these estimates of AGB_C from the undisturbed IFLs were also assumed to be reflective of AGB_P. The total number of GLAS shots available for subsequent modeling of AGB_P postfiltering was 25.1 million (47%; *SI Appendix*, Table S10). Separate random forest models were again developed for each of the six ecoregional realms referenced above (*SI Appendix*, Fig. S11). Prior to model calibration, 20% of the pixels in each realm were withheld for accuracy assessment. Additional methods details as well as an assessment of model performance, error, and uncertainty can be found in *SI Appendix*.

Map validation. Plot-based estimates of AGB were obtained from the Smithsonian Institution's Global Forest Carbon database (65) for the purposes of validating the AGB_P map product. Data from 1,108 field plots were obtained for forest stands ≥100 y old. Of these, 746 stands were ≥150 y old, and 591 stands were ≥200 y old. Seven plots were removed from consideration because the coordinate location did not match the country of origin. The AGB value associated with each of the remaining 1,101 samples was assumed to represent potential AGB for that location (*SI Appendix*, Fig. S12). For each country (66) and biome (Terrestrial Ecosystems of the World; TEOW) (59) containing a minimum of four plots, plot- versus map-based mean values of AGB_P were compared using the Pearson product-moment correlation (*r*). Map-based means were calculated using all pixel values (majority rule) within a 2-km buffer of each plot in each country or biome.

Potential aboveground carbon (RCP8.5). The maps of current and potential carbon storage described above were developed with climate variables reflecting baseline climate (ca. 1960 to 1990 average) conditions. However, climate change is likely to impact both the magnitude and spatial distribution of NCS opportunities for increasing carbon storage in biomass on land (i.e., AGB + BGB) as predicted under baseline climate conditions. To assess this risk of future

change in carbon storage, we first reran our model of AGB$_P$ under projected climate conditions by swapping out the WorldClim 1.4 baseline (1960 to 1990 average) climate variables for their WorldClim 1.4-projected counterparts under each of 11 global climate models (bcc-csm1-1, ccsm4, giss-e2-r, hadgem2-ao, hadgem2-es, ipsl-cm5a-lr, miroc-esm-chem, miroc-esm, miroc5, mri-cgcm3, and noresm1-m) for the high-emissions RCP8.5 by 2050. This resulted in 11 spatially explicit estimates of AGB$_P$ under RCP8.5, from which a mean estimate was computed using pixel-level raster math (*SI Appendix*, Fig. S1).

Belowground Carbon Storage.

Current and potential belowground carbon in biomass. Carbon density in BGB was estimated by applying published root:shoot ratios to the maps of AGB$_C$ and AGB$_P$ described above. Biome-level root:shoot ratios were compiled from previous research (67, 68) and were assigned spatially, first at the scale of TEOW biomes and then, as appropriate, at the scale of TEOW ecoregions within biomes (59). The result was a global vector-based map of ecoregional root:shoot ratios (*SI Appendix*, Fig. S13). The map was subsequently rasterized and reprojected to match the approximately 500-m (MODIS) sinusoidal grid of the AGB$_C$ and AGB$_P$ datasets using nearest-neighbor resampling. Raster multiplication was then used to generate separate maps of BGB$_C$ and BGB$_P$, including baseline climate and RCP8.5. In rare cases where ecoregional root:shoot assignments could not be readily made, BGB(y) was calculated according to

$$y = 0.489x^{0.890} \tag{2.3}$$

where a simple power function is applied to AGB(x) before multiplying by a generalized root:shoot ratio for forests and woodlands (67).

Current and potential belowground carbon in soil. Sanderman et al. (69) estimated the amount and spatial distribution of SOC in current (ca. 2010) and historic (no land-use scenario) stocks using a machine learning-based model calibrated with a global compilation of SOC observations collated by the International Soil Resource and Information Center. Current SOC density was predicted as a function of land use [fraction of a grid cell occupied by 1 of 11 land-use categories from Klein Goldewijk et al. (70)]; climatic, topographic, geologic, and landform characteristics; and depth at a spatial resolution of 10 km. Historic SOC density was then predicted using the same trained model but scaling back current land use to zero for all land-use categories. Consistent with the modeling of AGB$_P$, reflectance information was removed from the predictor stack. For the purposes of this study, maps of current and historic SOC density in the upper 2 m of soil were used and are hereafter referred to as current (SOC$_C$) and potential (SOC$_P$), respectively. In the original analysis of Sanderman et al. (69), a small portion of the land area showed apparent gains in SOC with the onset of agricultural activities. These areas were largely confined to irrigated regions of arid and semiarid landscapes. Rather than allow for the potential SOC to be lower than the current SOC in these cases, here, we set SOC$_P$ to be equal to SOC$_C$. The SOC$_C$ and SOC$_P$ raster layers were reprojected to match the approximately 500-m (MODIS) grid of the AGB$_C$ and AGB$_P$ datasets using nearest-neighbor resampling. Note that the estimate of SOC$_P$ produced by Sanderman et al. (69) reflects baseline climate conditions. No RCP8.5 analog was available for use in this study.

Unrealized Potential Carbon Storage.

The unrealized potential carbon storage, defined here as the difference between current and potential carbon storage, was calculated separately for AGB, BGB, and SOC and is denoted as AGB$_{UP}$, BGB$_{UP}$, and SOC$_{UP}$, respectively. In some cases, current carbon storage was estimated to be greater than the potential (AGB = 3.7%, BGB = 3.2%, and SOC = 2.6% of total pixels, respectively). This situation can occur, for example, in places where fire suppression has resulted in atypical levels of carbon accumulation. In these instances, we set the value of the corresponding pixel in the unrealized potential carbon storage layer to zero to make clear that no additional carbon opportunity exists in these locations.

Applying Societal Constraints.

The total unrealized potential carbon storage reflects the aggregate land carbon deficit, but this theoretical reservoir includes land that is currently essential for food production and human habitation, among other societally relevant values and services, and, thus, is not wholly available for the implementation of NCS. We, therefore, applied a series of spatially explicit constraints or safeguards to the unrealized potential data layer (*SI Appendix*, Fig. S2). First, we removed croplands from the unrealized potential layer using the Global Food Security support Analysis Data (GFSAD30) (*SI Appendix*, Fig. S2). Second, we removed permanent pasture using data from Ramankutty et al. (71), who produced a global pasture product (ca. 2000) using a combination of agricultural inventory and satellite-derived land cover data. Lastly, we masked out areas of high human population density (>300 people per km^2) using the Global Human Settlement Layer dataset (72), which is derived from the integration of 1) built-up areas extracted from Landsat imagery and 2) human population taken from the Gridded Population of the World version 4 dataset (73) (*SI Appendix*, Fig. S2). Additional detail on the data masking procedure can be found in *SI Appendix*.

Defining the NCS Opportunity.

We developed a data-driven conceptual model for differentiating what we hereafter refer to as the NCS opportunity space (Fig. 1). This model is intended to serve as an example of a data-driven approach to quantitatively disaggregating our spatial data by specific NCS interventions; however, alternative schemes could be devised. Our NCS opportunity space is two-dimensional, defined by axes representing current (x axis) and potential (y axis) carbon storage, which we then disaggregated into seven NCS opportunity categories (Fig. 1). We evaluate this opportunity space separately for three major bioclimate zones (boreal/polar, temperate, and tropics/subtropics) based on the Global Ecological Zones (GEZ; *SI Appendix*, Fig. S3) of the Food and Agriculture Organization of the United Nations (74). The GEZ dataset was acquired as an Esri (polygon) shapefile and rasterized to match the spatial resolution (approximately 500 m) and MODIS sinusoidal projection of the carbon density layers. For our purposes, the polar and boreal zones and the tropical and subtropical zones were combined, resulting in three bioclimate zones (*SI Appendix*, Fig. S3).

We identified two carbon-based thresholds for each bioclimate zone to separate areas with the potential to be 1) closed forests, 2) open forests, and 3) nonwoody systems (e.g., grasslands). In carbon terms, these categories roughly distinguish regions of high, medium, and low/no potential woody carbon, respectively. We refer to the threshold separating no/low potential woody carbon from all other woody systems as the "biotic threshold" (T$_B$) (Fig. 1; *SI Appendix*, Fig. S14). We refer to the threshold separating closed and open forest systems as the "forestry threshold" (T$_F$) (Fig. 1; *SI Appendix*, Fig. S15), so named as it coarsely differentiates woody-dominated systems into those with high suitability for forestry based NCS (*H*) and those with low suitability (*L*) (see *SI Appendix*, Table S9 for relevant NCS pathways). Additional information on the definition of T$_B$ and T$_F$ can be found in *SI Appendix*.

We identified three broad NCS activity types: restoration, management, and maintenance. Restoration refers to increasing carbon sinks through the expansion of native woody vegetation, management refers to the enhancement of woody carbon sinks through improved practices, and maintenance refers to preventing the loss of existing woody carbon sinks. We use this framework, adapted from Griscom et al. (6, 8), to further differentiate unrealized potential carbon in woody systems (i.e., open and closed forests) in terms of NCS opportunity. We use the ratio of current to potential (C:P) carbon storage to establish thresholds for subjectively defining these opportunity categories (Fig. 1). Ratios near zero (i.e., where current stocks are well below their potential) require restoration of carbon stocks, whereas ratios near one (i.e., where current stocks are near their potential) call for maintenance of carbon stocks. For our purposes, we deem restoration (*R*) to be required where current carbon storage is less than or equal to 25% of its potential (i.e., C:P ≤ 0.25) (Fig. 1). Conversely, we identify maintenance (*M*) as the most appropriate course of action where current carbon storage is within 10% of its potential (i.e., C:P > 0.90). For the remaining grid cells (i.e., where current carbon storage is between 25 and 90% of its potential; C:P of >0.25 but ≤0.90), we suggest a strategy for woody carbon enhancement that combines *MM* activities. Because our analysis is focused on the NCS opportunity afforded by woody carbon, we leave the nonwoody systems category undifferentiated.

We used the NCS opportunity space delineations described above (i.e., Fig. 1) to map the global distribution of the seven NCS opportunity categories (Fig. 2*A*). We then used raster-based zonal statistics to quantify the magnitude of the unrealized potential for land carbon storage afforded by each category in each bioclimate zone and by country in each zone.

Data Availability.

Data and code can be accessed at Harvard Dataverse (https://doi.org/10.7910/DVN/DSDDQK).

1. J. Rogelj et al., "Mitigation Pathways Compatible with 1.5°C in the Context of Sustainable Development" in Global Warming of 1.5°C. An IPCC Special Report on the Impacts of Global Warming of 1.5°C above Pre-Industrial Levels and Related Global Greenhouse Gas Emission Pathways, in the Context of Strengthening the Global Response to the Threat of Climate Change, Sustainable Development, and Efforts to Eradicate Poverty, V. Masson-Delmotte et al., Eds. (Intergovernmental Panel on Climate Change, 2018).
2. H. D. Matthews et al., An integrated approach to quantifying uncertainties in the remaining carbon budget. Commun. Earth Environ. 2, 7 (2021).
3. G. Grassi et al., Critical adjustment of land mitigation pathways for assessing countries' climate progress. Nat. Clim. Chang. 11, 425–434 (2021).
4. P. Smith et al., Biophysical and economic limits to negative CO2 emissions. Nat. Clim. Chang. 6, 42–50 (2016).
5. C. B. Field, K. J. Mach, Rightsizing carbon dioxide removal. Science 356, 706–707 (2017).
6. B. W. Griscom et al., Natural climate solutions. Proc. Natl. Acad. Sci. U.S.A. 114, 11645–11650 (2017).
7. J. E. Fargione, et al., Natural climate solutions for the United States. Sci. Adv. 4, eaat1869 (2018).
8. B. W. Griscom et al., National mitigation potential from natural climate solutions in the tropics. Philos. Trans. R. Soc. Lond. B Biol. Sci. 375, 20190126 (2020).
9. S. L. Lewis, C. E. Wheeler, E. T. A. Mitchard, A. Koch, Restoring natural forests is the best way to remove atmospheric carbon. Nature 568, 25–28 (2019).
10. S. Roe et al., Contribution of the land sector to a 1.5°C world. Nat. Clim. Chang. 9, 817–828 (2019).
11. K. M. Strassmann, F. Joos, G. Fischer, Simulating effects of land use changes on carbon fluxes: Past contributions to atmospheric CO2 increases and future commitments due to losses of terrestrial sink capacity. Tellus B Chem. Phys. Meterol. 60, 583–603 (2008).
12. J. Olofsson, T. Hickler, Effects of human land-use on the global carbon cycle during the last 6,000 years. Veg. Hist. Archaeobot. 17, 605–615 (2008).
13. R. S. DeFries, C. B. Field, I. Fung, G. J. Collatz, L. Bounoua, Combining satellite data and biogeochemical models to estimate global effects of human-induced land cover change on carbon emissions and primary productivity. Global Biogeochem. Cycles 13, 803–815 (1999).
14. R. A. Houghton, "Historic Changes in Terrestrial Carbon Storage" in Recarbonization of the Biosphere: Ecosystems and the Global Carbon Cycle, R. Lal, K. Lorenz, R. F. Hüttl, B. U. Schneider, J. von Braun, Eds. (Springer Netherlands, 2012), pp. 59–82.
15. J. Pongratz, C. H. Reick, T. Raddatz, M. Claussen, Effects of anthropogenic land cover change on the carbon cycle of the last millennium. Glob. Biogeochem. Cycles 23, GB4001 (2009).
16. E. Shevliakova, et al., Carbon cycling under 300 years of land use change: Importance of the secondary vegetation sink. Glob. Biogeochem. Cycles 23, GB2002 (2009).
17. R. A. Houghton, A. A. Nassikas, Global and regional fluxes of carbon from land use and land cover change 1850–2015. Global Biogeochem. Cycles 31, 456–472 (2017).
18. J. O. Kaplan et al., Holocene carbon emissions as a result of anthropogenic land cover change. Holocene 21, 775–791 (2010).
19. K. H. Erb et al., Unexpectedly large impact of forest management and grazing on global vegetation biomass. Nature 553, 73–76 (2018).
20. J.-F. Bastin et al., The global tree restoration potential. Science 365, 76–79 (2019).
21. A. Baccini et al., Tropical forests are a net carbon source based on aboveground measurements of gain and loss. Science 358, 230–234 (2017).
22. D. A. Bossio et al., The role of soil carbon in natural climate solutions. Nat. Sustain. 3, 391–398 (2020).
23. Y. Li et al., Local cooling and warming effects of forests based on satellite observations. Nat. Commun. 6, 6603 (2015).
24. P. M. Mykleby, P. K. Snyder, T. E. Twine, Quantifying the trade-off between carbon sequestration and albedo in midlatitude and high-latitude North American forests. Geophys. Res. Lett. 44, 2493–2501 (2017).
25. M. S. Balshi et al., Vulnerability of carbon storage in North American boreal forests to wildfires during the 21st century. Glob. Change Biol. 15, 1491–1510 (2009).
26. C. R. Schwalm, S. Glendon, P. B. Duffy, RCP8.5 tracks cumulative CO2 emissions. Proc. Natl. Acad. Sci. U.S.A. 117, 19656–19657 (2020).
27. B. M. Rogers, J. K. Balch, S. J. Goetz, C. E. R. Lehmann, M. Turetsky, Focus on changing fire regimes: Interactions with climate, ecosystems, and society. Environ. Res. Lett. 15, 030201 (2020).
28. W. R. L. Anderegg et al., Climate-driven risks to the climate mitigation potential of forests. Science 368, eaaz7005 (2020).
29. P. Olofsson et al., Good practices for estimating area and assessing accuracy of land change. Remote Sens. Environ. 148, 42–57 (2014).
30. J.-F. Bastin et al., Response to Comments on "The global tree restoration potential". Science 366, eaay8108 (2019).
31. S. L. Lewis, E. T. A. Mitchard, C. Prentice, M. Maslin, B. Poulter, Comment on "The global tree restoration potential". Science 366, eaaz0388 (2019).
32. W. Ruddiman, J. Kutzbach, S. Vavrus, Can natural or anthropogenic explanations of late Holocene CO2 and CH4 be falsified? Holocene 21, 865–8879 (2011).
33. J. E. M. Watson et al., The exceptional value of intact forest ecosystems. Nat. Ecol. Evol. 2, 599–610 (2018).
34. S. C. Cook-Patton et al., Mapping carbon accumulation potential from global natural forest regrowth. Nature 585, 545–550 (2020).
35. P. Fearnside, "Deforestation of the Brazilian Amazon" in Oxford Research Encyclopedia (Oxford University Press, 2017).
36. H. Escobar, Deforestation in the Amazon is shooting up, but Brazil's president calls the data 'a lie.' Science (2019) doi:10.1126/science.aay9103.
37. INPE, Earth observation general coordination, Monitoring Program of the Amazon and other biomes. Deforestation - Legal Amazon (2019) (April 23, 2020).
38. C. J. Nolan, C. B. Field, K. J. Mach, Constraints and enablers for increasing carbon storage in the terrestrial biosphere. Nat. Rev. Earth Environ. 2, 436–446 (2021).
39. S. Roe et al., Land-based measures to mitigate climate change: Potential and feasibility by country. Glob. Change Biol. 27, 6025–6058 (2021).
40. C. R. Schwalm et al., Modeling suggests fossil fuel emissions have been driving increased land carbon uptake since the turn of the 20th Century. Sci. Rep. 10, 9059 (2020).
41. A. J. Winkler et al., Slowdown of the greening trend in natural vegetation with further rise in atmospheric\chemCO_2. Biogeosciences 18, 4985–5010 (2021).
42. P. Friedlingstein et al., Uncertainties in CMIP5 climate projections due to carbon cycle feedbacks. J. Clim. 27, 511–526 (2014).
43. K. Zhu, J. Zhang, S. Niu, C. Chu, Y. Luo, Limits to growth of forest biomass carbon sink under climate change. Nat. Commun. 9, 2709 (2018).
44. L. V. Gatti et al., Amazonia as a carbon source linked to deforestation and climate change. Nature 595, 388–393 (2021).
45. K. A. Duffy et al., How close are we to the temperature tipping point of the terrestrial biosphere? Sci. Adv. 7, eaay1052 (2021).
46. N. G. McDowell et al., Pervasive shifts in forest dynamics in a changing world. Science 368, eaaz9463 (2020).
47. A. Koch, C. Brierley, S. L. Lewis, Effects of Earth system feedbacks on the potential mitigation of large-scale tropical forest restoration. Biogeosciences 18, 2627–2647 (2021).
48. K. Zickfeld, D. Azevedo, S. Matheius, H. D. Matthews, Asymmetry in the climate–carbon cycle response to positive and negative CO2 emissions. Nat. Clim. Chang. 11, 613–617 (2021).
49. S. C. Cook-Patton et al., Protect, manage and then restore lands for climate mitigation. Nat. Clim. Chang. 11, 1027–1034 (2021).
50. D. J. Zarin et al., Can carbon emissions from tropical deforestation drop by 50% in 5 years? Glob. Change Biol. 22, 1336–1347 (2016).
51. W. S. Walker et al., The role of forest conversion, degradation, and disturbance in the carbon dynamics of Amazon indigenous territories and protected areas. Proc. Natl. Acad. Sci. U.S.A. 117, 3015–3025 (2020).
52. A. Baccini et al., Estimated carbon dioxide emissions from tropical deforestation improved by carbon-density maps. Nat. Clim. Chang. 2, 182–185 (2012).
53. N. L. Harris et al., Global maps of twenty-first century forest carbon fluxes. Nat. Clim. Chang. 11, 234–240 (2021).
54. M. Chapman et al., Large climate mitigation potential from adding trees to agricultural lands. Glob. Change Biol. 26, 4357–4365 (2020).
55. R. J. Hijmans, S. E. Cameron, J. L. Parra, P. G. Jones, A. Jarvis, Very high resolution interpolated climate surfaces for global land areas. Int. J. Climatol. 25, 1965–1978 (2005).
56. T. Hengl et al., SoilGrids250m: Global gridded soil information based on machine learning. PLoS One 12, e0169748 (2017).
57. USGS, GTOPO30 https://www.usgs.gov/centers/eros/science/usgs-eros-archive-digital-elevation-global-30-arc-second-elevation-gtopo30. Accessed 18 September 2018.
58. T. G. Farr et al., The Shuttle Radar Topography Mission. Rev. Geophys. 45, RG2004 (2007).
59. E. Dinerstein et al., An ecoregion-based approach to protecting half the terrestrial realm. Bioscience 67, 534–545 (2017).
60. CIESIN, ITOS, Global Roads Open Access Data Set, Version 1 (gROADSv1). (2013).
61. M. C. Hansen et al., High-resolution global maps of 21st-century forest cover change. Science 342, 850–853 (2013).
62. M. A. Friedl et al., MODIS Collection 5 global land cover: Algorithm refinements and characterization of new datasets. Remote Sens. Environ. 114, 168–182 (2010).
63. ESRI, Digital chart of the world: For use with ESRI desktop software (1994).
64. P. Potapov et al., Mapping the world's intact forest landscapes by remote sensing. Ecol. Soc. 13, 51 (2008).
65. K. J. Anderson-Teixeira et al., ForC: A global database of forest carbon stocks and fluxes. Ecology 99, 1507–1507 (2018).
66. GADM, Global administrative areas (boundaries). https://gadm.org/. Accessed 1 November 2018.
67. K. Mokany, R. J. Raison, A. S. Prokushkin, Critical analysis of root:shoot ratios in terrestrial biomes. Glob. Change Biol. 12, 84–96 (2006).
68. J. Hutchison, A. Manica, R. Swetnam, A. Balmford, M. Spalding, Predicting Global Patterns in Mangrove Forest Biomass. Conserv. Lett. 7, 233–240 (2014).
69. J. Sanderman, T. Hengl, G. J. Fiske, Soil carbon debt of 12,000 years of human land use. Proc. Natl. Acad. Sci. U.S.A. 114, 9575–9580 (2017).
70. K. Klein Goldewijk, A. Beusen, G. Drecht, M. Vos, The HYDE 3.1 spatially explicit database of human-induced global land-use change over the past 12,000 years. Glob. Ecol. Biogeogr. 20, 73–86 (2011).
71. N. Ramankutty, A. T. Evan, C. Monfreda, J. A. Foley, Farming the planet: 1. Geographic distribution of global agricultural lands in the year 2000. Glob. Biogeochem. Cycles 22 (2008).
72. M. Pesaresi, S. Freire, GHS-SMOD R2016A - GHS settlement grid, following the REGIO model 2014 in application to GHSL Landsat and CIESIN GPW v4-multitemporal (1975-1990-2000-2015). https://ghsl.jrc.ec.europa.eu/. Accessed 8 July 2019.
73. CIESIN, Gridded Population of the World, Version 4 (GPWv4): Population Density, Revision 11 (2018). https://sedac.ciesin.columbia.edu/data/collection/gpw-v4. Accessed 19 June 2019.
74. Food and Agriculture Organization, Global Ecological Zones, ed. 2, 2013. https://www.fao.org/nr/gaez/en/. Accessed 26 August 2018.